Strain-Dependent Modulation of Phosphate Transients in Rabbit Skeletal Muscle Fibers

Earl Homsher,* Joan Lacktis,* and Michael Regnier#
*Department of Physiology, University of California at Los Angeles, Los Angeles, California 90024, and #Department of Physiology and Biophysics, University of Washington, Seattle, Washington 98195 USA

ABSTRACT When inorganic phosphate (P_i) is photogenerated from caged P_i during isometric contractions of glycerinated rabbit psoas muscle fibers, the released P_i binds to cross-bridges and reverses the working stroke of cross-bridges. The consequent force decline, the P_i-transient, is exponential and probes the kinetics of the power-stroke and P_i release. During muscle shortening, the fraction of attached cross-bridges and the average strain on them decreases (Ford, L. E., A. F. Huxley, and R. M. Simmons, 1977. Tension responses to sudden length change in stimulated frog muscle fibers near slack length. *J. Physiol. (Lond.).* 269:441–515; Ford, L. E., A. F. Huxley, and R. M. Simmons, 1985. Tension transients during steady state shortening of frog muscle fibers. *J. Physiol. (Lond.).* 361:131–150. To learn to what extent the P_i transient is strain dependent, muscle fibers were activated and shortened or lengthened at a fixed velocity during the photogeneration of P_i. The P_i transients observed during changes in muscle length showed three primary characteristics: 1) during shortening the P_i transient rate, k_{Pi}, increased and its amplitude decreased with shortening velocity; k_{Pi} increased linearly with velocity to >110 s^{-1} at 0.3 muscle lengths per second (ML/s). 2) At a specific shortening velocity, increases in $[P_i]$ produce increases in k_{Pi} that are nonlinear with $[P_i]$ and approach an asymptote. 3) During forced lengthening k_{Pi} and the amplitude of the P_i transient are little different from the isometric contractions. These data can be approximated by a strain-dependent three-state cross-bridge model. The results show that the power stroke's rate is strain-dependent, and are consistent with biochemical studies indicating that the rate-limiting step at low strains is a transition from a weakly to a strongly bound cross-bridge state.

INTRODUCTION

Because the release of inorganic phosphate (P_i) from AM.ADP.P_i[1] is associated with a large free energy change, it has been suggested that the release of P_i is directly associated with force generation during the cross-bridge cycle (White and Taylor, 1976; Eisenberg et al., 1980; Sleep and Hutton, 1978; Hibberd et al., 1985). There are three lines of evidence, however, that suggest the release of P_i *follows* a force-producing isomerization of the AM.ADP.P_i state. First, if a fully activated isometrically contracting muscle is pressurized to 10 MPa, the force is reduced by ~8%. When the pressure is rapidly reduced to an atmospheric value, force increases with a rate constant of ~20–30 s^{-1} without a change in the $I_{1,1}/I_{1,0}$ x-ray diffraction ratio (Knight et al., 1993; Fortune et al., 1991). Additionally, the rate of this force rise increases in a nonlinear saturating fashion as $[P_i]$ rises, consistent with the existence of a force-generating cross-bridge isomerization before the release of P_i (Fortune et al., 1994). Second, force produced by isometrically contracting muscles is reduced following the photogeneration of P_i from 1-(2-nitrophenyl)ethylphosphate (caged P_i). These studies show that force decays at a rate that increases nonlinearly and asymptotically with $[P_i]$. This behavior again is inconsistent with a single force-generating step directly produced by a P_i release (Dantzig et al., 1992; Millar and Homsher, 1990; Walker et al., 1992.) Furthermore, there is a 1–4-ms lag after the P_i release and preceding force decay, which is also inconsistent with P_i binding directly reversing the force-producing step. Finally, using sinusoidal analysis, Kawai and collaborators (Kawai and Halvorson, 1991; Kawai and Zhao, 1993; Zhao and Kawai, 1994) have shown that the ratio of stress change to strain change in the frequency domain can be described by four processes (A–D). Their exponential process B also exhibits a hyperbolic dependence on $[P_i]$ that is similar to that observed in the pressure-jump and $[P_i]$-jump studies. Kawai and Halvorson (1991) have also interpreted their data as indicative of the presence of a force-generating isomerization preceding release of P_i. A weakness common to these approaches is that, aside from the work on the P_i transient (Dantzig et al., 1992), the data were interpreted using strain independent kinetic models, as is done in solution studies. However, the nonlinear dependence of the rate of ATP hydrolysis and heat+work production on muscle shortening velocity (Woledge et al., 1985) and the rapid tension transients seen during rapid releases and stretches (Ford et al., 1977) suggest the cross-bridge cycle kinetics are strongly influenced by cross-bridge strain.

Attempts to model the cross-bridge cycle during different mechanical states have relied heavily on strain-dependent rate constants to approximate the cross-bridge behavior (Eisenberg et al., 1980; Pate and Cooke, 1989a; Smith and Geeves, 1995). Since P_i transients reflect the cross-bridge

Received for publication 3 July 1996 and in final form 13 January 1997.
Address reprint requests to Dr. Earl Homsher, Dept. of Physiology, School of Medicine, University of California, Los Angeles, CA 90024. Tel.: 310-825-6976; Fax: 310-206-5661; E-mail: ehomsher@physiology.med-sch.ucla.edu.

[1] AM.ADP.P_i is a quarternary complex of actin (A), myosin (M), ADP, and P_i (inorganic phosphate) formed after the hydrolysis of ATP.

0006-3495/97/04/1780/12 $2.00

transitions associated with force generation, insight might be gained about the strain dependence of these processes by characterizing the dependence of the P_i transient on mechanical strain. Thus, in the work described below, P_i transients were measured in muscle fibers during steady-state shortening at various velocities. We assume that during shortening, the average strain exerted by cross-bridges is reduced. We hypothesize that the effect of the reduced strain will be manifest in changes in the P_i transient rate and amplitude. In the experiments described below, single muscle fibers, equilibrated in caged P_i, were maximally activated under isometric conditions. The fibers were then allowed to shorten at various velocities, and as steady-state force was approached, P_i was photogenerated and the resultant decline in force (P_i transient) monitored. These experiments revealed that during shortening, the rate of the phosphate transient, k_{Pi}, increases in almost linear proportion to the shortening velocity. Furthermore, the amplitude of the P_i transient (Amp_{Pi}) is reduced by shortening and to a greater extent than the reduction in steady-state force produced by shortening. This result suggests that there are more than one force-bearing state in the muscle, and that during shortening, the force exerting AM.ADP state that binds P_i is reduced to a greater extent than is force. Finally, at a fixed shortening velocity, k_{Pi} exhibits a hyperbolic relationship with respect to $[P_i]$ similar to that seen in the isometric contractions. These results can be approximated by an extension of the strain-dependent model used in earlier work (Dantzig et al., 1992). The general significance of these experiments is that they seriously limit the strain dependency one may use in cross-bridge models. Preliminary results from these studies have been reported (Homsher and Lacktis, 1988).

MATERIALS AND MATERIALS

Solutions

All fiber solutions were maintained at 200 mM ionic strength (at pH 7.1 and 10°C) and contained (in mM) 100 *N,N*-bis[2-hydroxyethyl-2-aminoethanesulfonic acid, 6 MgATP, 1 Mg^{2+} (added as magnesium acetate), 20 potassium acetate, 20 EGTA, and 15 creatine phosphate, as well as 200 U/ml creatine phosphokinase (Sigma, St. Louis, MO). Preactivation solutions contained 2 mM EGTA and 18 mM HDTA. For activation solutions, the ratio of Ca^{2+}-EGTA/K_2EGTA was adjusted to obtain a pCa of 4.5 while holding the total EGTA content fixed at 20 mM. The $[P_i]$ of preactivation and activation solutions was adjusted by reducing potassium acetate and adding potassium phosphate at pH 7.1. All solutions contained contaminating P_i from breakdown of ATP and creatine phosphate in stock solutions. The contamination level of P_i was assumed to be 0.7 mM (Millar and Homsher, 1990) and is reflected in the P_i reported in the text. For caged P_i solutions, preactivation and activation solutions contained 5 mM caged P_i and 10 mM dithiothreitol. Caged P_i was synthesized and purified as described previously (Dantzig et al., 1992). Contamination by $[P_i]$ in the caged P_i was <2% and this contaminating P_i, as well as caged P_i binding to cross-bridges, reduced force in activated fibers by ~10% (Dantzig et al., 1992). The sequence of fiber exposure to the relaxing, preactivation, and activation solutions were as previously described (Dantzig et al., 1992).

Mechanical measurements

Psoas muscle fibers from female New Zealand White rabbits were demembranated by a glycerol-extraction method (Goldman et al., 1984), stored at −20°C, and used for up to 6 weeks. Procedures for mounting short (2.5–4.7 mm) lengths of fiber using t-clips, thermostating (all experiments were at 10 ± 0.5°C), exchanging solutions, and making force and sarcomere length measurements were as previously described (Dantzig et al., 1992). One end of a fiber was attached to either a Cambridge Technology 400 (Cambridge, MA) or SensoNor AE801 strain gauge (Horten, Norway) for force measurements, while the other was attached to a length driver (Ling 100A shaker motor) (Homsher and Rall, 1973). The servo-controlled length driver allows for length maintenance, isovelocity-ramp shortening or stretching, or variable-length quick releases (up to 300 μm displacement in <2 ms) followed by a variable isovelocity displacement. Sarcomere length was generally set at 2.7–2.8 μm/sarcomere, but for experiments in which muscles were forcibly lengthened, the initial length was reduced to 2.5 μm.

Photolysis of caged P_i

The $[P_i]$ in fibers was rapidly increased by photolysis of caged P_i using a frequency-doubled dye laser (UV-500, Candela, Bedford, MA). The frequency-doubled secondary beam was isolated and focused onto the fiber by passing through WG305 and UG11 filters and a plano-convex cylindrical fused silica lens (focal length = 10 cm). The fibers were carefully masked with stainless steel sheets positioned 2 mm above the fiber so that the laser beam could not strike the t-clips used to attach the muscle fiber to the transducer hooks. Control experiments in fibers in solutions without caged compounds showed that the laser pulse produced no thermal or light noise on resting or fully activated force records. A detailed description of the methods for photolysis of caged P_i, using the frequency-doubled dye laser, is provided in an earlier publication (Millar and Homsher, 1990). Before each experiment, the laser was adjusted to deliver 30 mJ of 320 nm light (measured by a Scientech 365 digital energy meter) so as to rapidly release 1 mM P_i from the 5 mM caged P_i activation solution. In several instances the energy was increased to 45 mJ to release 1.5 mM of P_i.

Data reduction

Data were acquired at 1–20 kHz and analyzed using the program KFIT (written by Dr. Neil Millar). This program also provides user-defined curve fits to the data by a nonlinear least-squares procedure with the use of a Marquardt technique (Press et al., 1986). All the P_i transients were fit to an equation of the form

$$Y = A1 + A2*(1 - \exp[-A3*t]) + A4*t \qquad (1)$$

where $A1$ is the starting force, $A2$ and $A3$ are the exponential amplitude and rate constant, respectively, and $A4$ is a constant slope. Fibers were excluded if the control level of isometric force decreased by >10% during the course of an experiment. Unloaded shortening velocity (V_u) was measured using the "slack-test" method (Edman, 1979). The experiments were performed in two series. V_u (referenced to a sarcomere length of 2.25 μm) measured in the first series averaged 1.90 ± 0.13 muscle lengths (ML)/s (n = 5), and in the second series, V_u was 2.15 ± 0.1 ML/s (n = 19). For experiments in which V_u was not measured it was assumed to be 2 ML/s.

Modeling was done using QBASIC programs written specifically to simulate a particular reaction sequence.

RESULTS

The effect of shortening on k_{Pi} and Amp_{Pi} during isovelocity shortening

Fig. 1 is a slow time-base recording of force production (*a, b*) and displacement (*c*) of a single muscle fiber that was

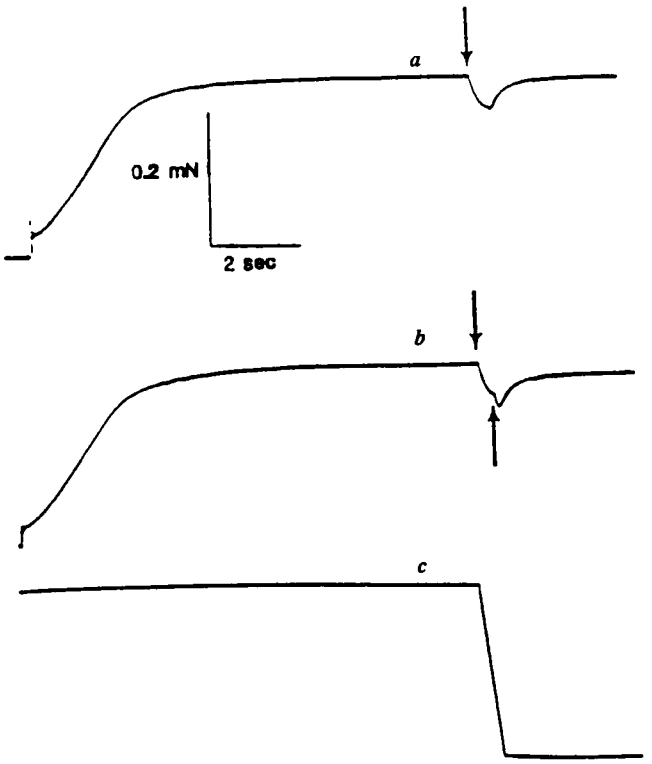

FIGURE 1 The time course of force (*a* and *b*) and shortening (*c*) on a slow time base. *a* is the tension of a control contraction in which the fiber was activated at pCa 4.5; shortening (at 0.1 ML/s, for a distance 156 μm (4% ML) in 0.4 s) begins (indicated by the *down arrow*) ~5 s after beginning of activation of the fiber. During shortening, force declines to 81% of the isometric value. At the end of shortening the muscle redevelops force to near maximal values. *b*, from the same fiber, behaves identically, except that 0.2 s after the beginning of shortening, the muscle is pulsed with a burst of laser energy to release P_i, subsequent to which force declines. The fiber is that used in Fig. 6.

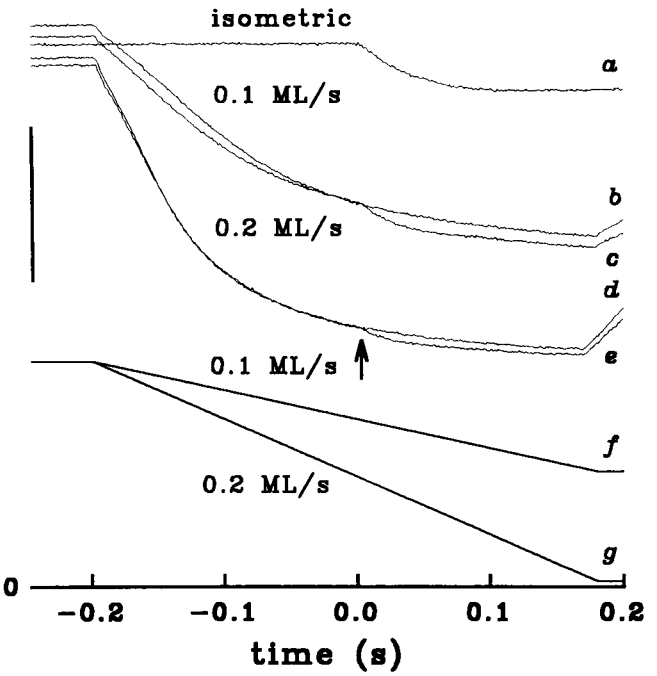

FIGURE 2 Superimposed force recordings and the response to a P_i jump by two muscle fibers contracting isometrically (*a*), shortening at 0.1 ML/s with (*c*) and without (*b*) a P_i jump, and shortening at 0.2 ML/s with (*e*), and without (*d*) a P_i jump. The displacement records for 0.1 ML/s and 0.2 ML/s are shown in traces *f* and *g*. P_i was liberated at the point indicated by the upward pointing arrow. The vertical bar to the left corresponds to 38 kN/m^2; the time base at the bottom corresponds to zero force and the numbers indicate the time in seconds before (negative) or after (positive) the laser flash. The maximal isometric force for this muscle was 233 kN/m^2, the fiber length was 3.49 mm at a sarcomere spacing of 2.80 μm. The rate of shortening in this case was 140 μm/0.4 s (0.1 ML/s), and 280 μm/0.4 s (0.2 ML/s). The force during shortening after the laser flash averaged 0.655 P_o (0.69–0.62 P_o) for the contraction at 0.1 ML/s and 0.475 P_o (0.495–0.455 P_o) at 0.2 ML/s. Fiber cross-sectional area = 6165 μm^2.

fully activated (in a solution containing 5 mM c-P_i). After force approached an isometric steady state, the fiber was allowed to shorten at a fixed velocity (0.1 ML/s in Fig. 1) for a distance of ~4.5% of the fiber's length. In record *a*, the control, force declines during shortening to nearly a steady value, and with the cessation of shortening, redevelops force to the preshortening level. In recording *b*, the same protocol as in *a* is used, but 200 ms after the beginning of shortening, the fiber was flashed (indicated by *upward arrow*) to release 1 mM P_i from c-P_i, which produced a rapid decline in force. Fig. 2 illustrates typical transients recorded on a faster time base for three specific cases: an isometric contraction during which P_i was photogenerated (*a*); two contractions (records *b* and *c*) in which the muscle shortened at a velocity of 0.1 ML/s (*b*), and when P_i was liberated during shortening (*c*); and two contractions similar to *b* and *c* with shortening at 0.2 ML/s (*d* and *e*). In the shortening contractions, e.g., at 0.1 ML/s, record *c* was shifted vertically so that the force traces would superimpose for the period before P_i was photoliberated; at 0.2 ML/s record *d* was lowered slightly to produce the same superimposition on record *e*. With this superimposition of records one can discern the effect of P_i liberation on the force. The five traces show the pattern typical in these experiments. In the isometric contraction, the generation of 1 mM P_i produced a 12% decrease in tension within 150–200 ms. With the fiber shortening at 0.1 ML/s, there was a smaller (~3% of the force in the isometric contraction) and faster (<100 ms) force decline. At a still higher shortening velocity (0.2 ML/s), the effect is even more pronounced; here the force decline is <2% of the isometric force and the transient is complete in <50 ms. This behavior is better seen in Fig. 3, which plots the *difference* between force produced by the shortening control and the paired shortening and "flashed" experimental contractions, normalized to the preflash force. This protocol compensates for the effects of shortening on force. In Fig. 3, the trace labeled *isometric* is the isometric control; the trace labeled 0.1 ML/s is the difference (*record b − record c* in Fig. 2) observed during shortening at 0.1 ML/s; and the trace labeled 0.2 ML/s is the difference (*record d − record e* in Fig. 2) seen at 0.2 ML/s. The results are unequivocal in that least-squares fits (indicated by the

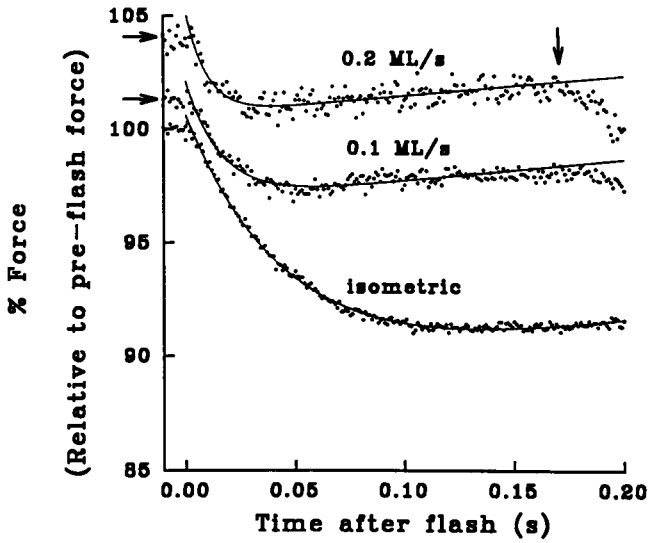

FIGURE 3 Plots of the P_i transients in the isometric and isovelocity at 0.1 ML/s and 0.2 ML/s from the data shown in Fig. 2. The force in each case is referenced to the force (P_f) immediately preceding the P_i transient (100%) and the arrows to the left of the figure designate the 100% value for each recording. The traces were slightly shifted vertically to simplify identification of the recordings. Solid lines are least-squares fits of the data by Eq. 1. The results of fitting of the data are as follows: for record isometric, starting point (st. pt., zero time) = 100.7%, Amp_{Pi} = −12.0%, and the rate constant for the exponential phase is 21.7 s^{-1}; for (0.1 ML/s), st. pt. = 101.2%, Amp_{Pi} = −5.4%, rate = 61.6 s^{-1}; for (0.2 ML/s), st. pt. = 101.4%, Amp_{Pi} = −4.7%, and rate = 106 s^{-1}.

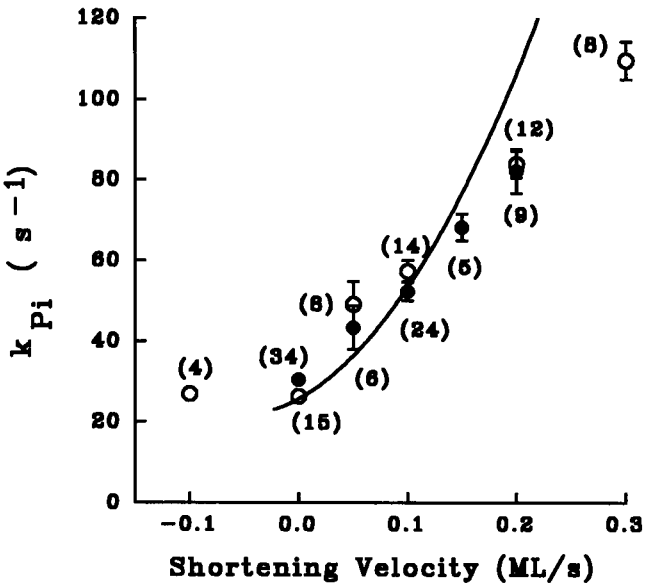

FIGURE 4 Plots of the averaged P_i transient rates during shortening at velocities given on the abscissa. The closed circles are from experiments in which the shortening was at fixed velocity throughout the shortening, while those in open circles were obtained using the sudden release to bring the force near the steady-state force before isovelocity shortening. The numbers in parentheses are the number of fibers from which the data were obtained, while the bars on either side of the data points are standard errors of the mean. The data from the two sets of experiments are so similar that they are fitted by single line whose linear least-squares fit is given by the equation k_{Pi} rate (in s^{-1}) = 29.8(±1.5) + 265(±10) × (shortening velocity (ML/s)), r^2 = 0.998. The solid line represents the k_{Pi} three-state strain-dependent model (see Discussion).

solid lines in Fig. 3) of exponential equations to the records show that the rate of the force decline, k_{Pi}, is markedly accelerated (from 21.7 s^{-1} in the isometric case to 106.2 s^{-1} at 0.2 ML/s) and reduced in size (Amp_{Pi}, from 12% of the preflash force to 4.7% of the preflash force) by muscle shortening at 0.2 ML/s. This type of experiment was performed over a range of velocities from 0.05–0.20 ML/s, and the results, analyzed as in Fig. 3, are summarized in Figs. 4 (k_{Pi}, *filled circles*) and 5 (Amp_{Pi}, *filled circles*). The averaged data indicate that as shortening velocity increases, there is a linear increase in k_{Pi} and a reciprocal fall in Amp_{Pi}.

A separate series of experiments were conducted in which isometric force was reduced to a predetermined value by a small quick (<2 ms) release followed by shortening at a constant velocity (e.g., 0.1 ML/s) to hold force constant. The results of these experiments are plotted as open circles in Figs. 4 and 5 and are indistinguishable from those obtained by isovelocity shortening alone. A linear extrapolation of the k_{Pi} versus shortening velocity suggests that at V_u, 2ML/s, k_{Pi} is >500 s^{-1} (not shown). Reliable measurements of the P_i transient rate at higher velocities were not possible, as the signal-to-noise ratio became too small for accurate resolution. The amplitudes of the isometric P_i transients in this series were smaller than those in the initial series and those reported earlier (Dantzig et al., 1992). However, isometric k_{Pi} and isovelocity k_{Pi} and Amp_{Pi} were not different, so that an increased contamination by P_i can not be the reason for the difference.

The effect of $[P_i]$ on k_{Pi} and Amp_{Pi} during shortening

Previous studies have shown that k_{Pi} increases as the $[P_i]$ increases, but the relationship is approximately hyperbolic and indicative of a saturating process (Dantzig et al., 1992; Walker et al., 1992). In the following series of experiments, we varied the initial $[P_i]$ concentration and again measured k_{Pi} and Amp_{Pi} in isometric and isovelocity shortening (0.1 ML/s) contractions. This velocity was selected because it approximately doubles k_{Pi} and the Amp_{Pi} is still relatively easy to measure. As the initial $[P_i]$ increases, force is reduced, decreasing the signal-to-noise ratio and making the effects more difficult to resolve. We therefore limited initial $[P_i]$ in the contraction solutions to 0.7 mM, 1.6 mM, 2.5 mM, or 4.3 mM P_i. Since these experiments required a large number of contractions (at least 17 contractions/relaxation cycles and 6 laser flashes), we did not obtain a complete series on any one muscle fiber. The records in Fig. 6 illustrate the basic results from a single fiber. Records *a* and *d* are isometric contractions at an initial P_i concentration of 0.7 and 2.5 mM P_i, respectively. At the arrow (defined as t = 0) an additional 1.5-mM P_i was photo-generated in the

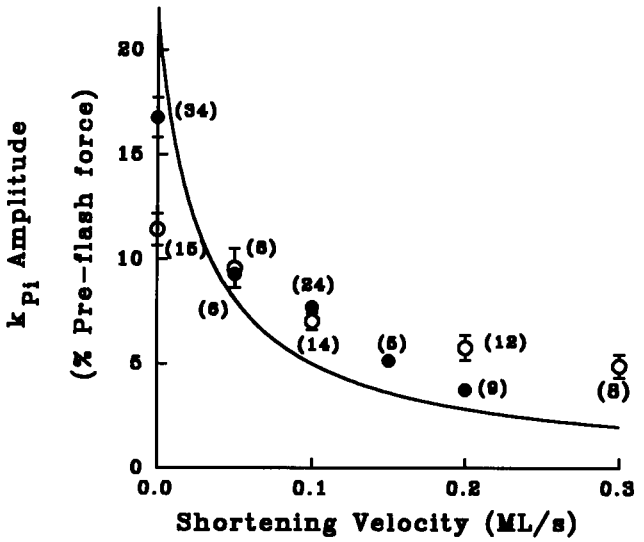

FIGURE 5 The effect of shortening velocity on the amplitude of the P_i-transient. The open circles are those data from experiments in which a quick release preceded isovelocity shortening (at the given velocity) and the closed circles are from the experiments in which velocity was constant throughout the shortening. The solid line is the prediction of P_i-transient amplitude predicted by the three-state strain-dependent model (see Discussion).

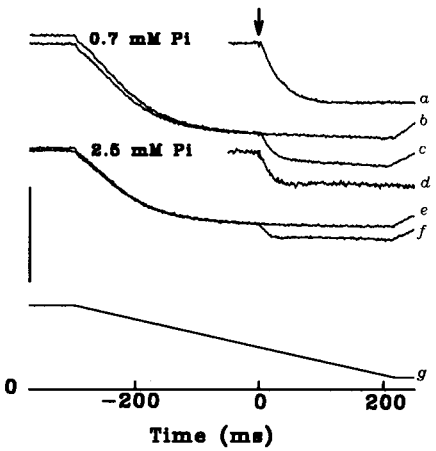

FIGURE 6 The effects of different $[P_i]$ on P_i transients while shortening at a fixed velocity of 0.1 ML/s (as represented in recording *g*). *a–c* were taken in a solution whose initial concentration was 0.7 mM P_i. Those for records *d–f* were in a solution whose initial $[P_i]$ = 2.5 mM. *a* and *d* are for isometric contractions while records *b–e* were shortening at a rate of 0.1 ML/s. The records for the lower initial $[P_i]$ were shifted upward slightly (~3% of the isometric force) and those at the high initial $[P_i]$ were shifted downward by ~15% of the isometric force to permit simple identification of the records. The isometric force at 2.5 mM $[P_i]$ averaged 85% of that at 0.7 mM $[P_i]$. The vertical bar to the left corresponds to 55 kN/m^2 for force records and 226 μm for displacement. The average force at 1 mM P_i was 172 kN/m^2 and at 2.5 mM P_i was 148 kN/m^2 in this fiber. The fiber dimensions are 3.41 mm long at 2.7 μm, with a cross-sectional area of 2502 μm^2. The steady-state force during shortening at 0.7 mM P_i was 0.738 P_o and was 0.727 P_o for that at 2.5 mM P_i.

fiber by a laser pulse. In the other fibers in this series, 1 mM P_i was photogenerated. Recordings *b* and *c* were initially at 0.7 mM P_i, but with isovelocity shortening of 0.1 ML/s [indicated by the displacement record (*g*)], an additional 1.5 mM P_i was generated at time 0 in contraction *c*. The results are comparable to those seen in Figs. 2 and 4. In records *e* and *f* the same muscle fiber was incubated in 2.5 mM P_i before contraction and shortening began. This reduced isometric force by 18% in *d–f* (as compared with *b* and *c*); an effect similar to that previously reported for this concentration of P_i (Dantzig et al., 1992). When the P_i transient is produced by photoliberation of P_i starting from a higher concentration (as in contraction *d*, compared with its control *a*), the Amp_{Pi} is reduced in size and is faster, as has been reported in earlier studies (Dantzig et al., 1992; Walker et al., 1992; Millar and Homsher, 1990). Similarly, a comparable effect is seen in the shortening muscle (record *f* as compared with *c*). This behavior is more clearly seen in the difference plots (*b* and *c* and *e–f*, see above) given in Fig. 7 *A* and *B*. In Fig. 7 *A* the isometric P_i transient (*a*) and isovelocity transient (*b*) occurring after the P_i increase from 0.7 mM to 2.2 mM exhibits the behavior observed in Fig. 3; in this case k_{Pi} increases from 31.6 s^{-1} (isometric) to 60.3 s^{-1} during shortening. In Fig. 7 *B* k_{Pi} at 0.1 ML/s and 4 mM final P_i increased from 65.2 s^{-1} in the isometric case to 103.1 s^{-1}. At the two different final P_i concentrations (2.2 mM and 4.0 mM), shortening increased k_{Pi} over the isometric value by ~35 s^{-1} and reduced the Amp_{Pi} to ~50% of its value in the isometric contraction. Fig. 8 summarizes the results of experiments at a series of different P_i concentrations and the photogeneration of 1 mM P_i. The data show that shortening at 0.1 ML/s increase k_{Pi} by roughly the same extent at each. Fits of the isometric k_{Pi} over this limited $[P_i]$ range to the equation $k_{Pi} = k_{+a} + k_{Pi}*[P_i]$, gave k_a = 22 s^{-1} and $k_{Pi} = 7.2 \times 10^3$ M^{-1} s^{-1} for the isometric case, and k_{+a} = 41 s^{-1} and $k_{Pi} = 6.6 \times 10^3$ M^{-1} s^{-1} for the isovelocity shortening. The isometric value compares well to the k_{+a} = 23 s^{-1} and $k_{Pi} = 6.2 \times 10^3$ M^{-1} s^{-1} over the same $[P_i]$ range for isometric contractions in the work of Dantzig et al. (1992).

The effect of isovelocity stretches on the k_{Pi} and Amp_{Pi}

Based on the data in Fig. 4, one might predict that at negative shortening velocities (forcible lengthening of the muscle), k_{Pi} might decrease. To see if this was so, several experiments were made in which the muscle fiber was forcibly lengthened at 0.1 ML/s during maximal contraction. These experiments were difficult in that fibers often broke during the repeated stretches needed for these experiments. Fig. 9 shows a successful experiment. Record *c* shows an isometric contraction with the photogeneration of P_i at zero time (*down arrow*). Record *a* is a control contraction with a sudden stretch followed by an isovelocity stretch, while record *b* is the same protocol *with* photogeneration of P_i. The results suggest that forcibly lengthening a muscle has relatively little effect on the P_i transient. The

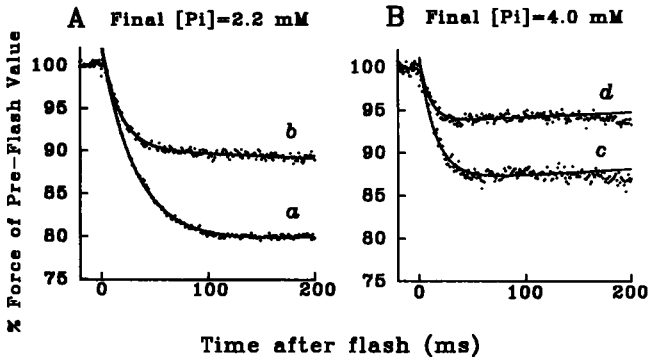

FIGURE 7 Plots of the time course of the P_i transient at final concentration of 2.2 and 4.0 mM [P_i] from the experiments shown in Fig. 6. (*A*) is at 2.2 mM P_i: *a*, the isometric P_i transient (data given by the dots) and *b*, shortening at 0.1 ML/s; (*B*) is 4.0 mM P_i; *c*, the isometric contraction, and *d* shortening at 0.1 ML/s. The solid line in each case is the least-squares fit to a single exponential with a sloping baseline. For *a* best fit data has a st. pt. of 102.3%, amplitude = −23.1%, and a rate of 31.6 s^{-1}; for *b*, st. pt. = 102.8%, amplitude = −2.6%, and a rate of 60.3 s^{-1}; for *c*, st. pt. = 101.2%, amplitude = −14.5%, and a rate of 65.2 s^{-1}; and for *d*, st. pt. = 101.2%, amplitude of −7.6%, and a rate of 103.1 s^{-1}.

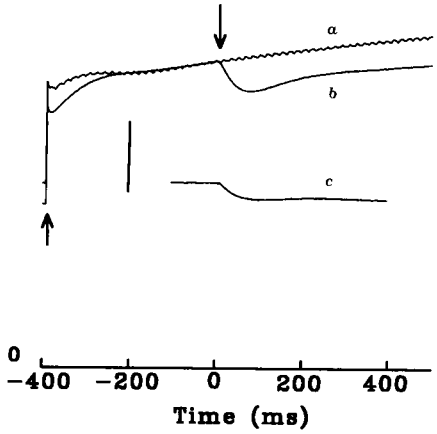

FIGURE 9 Plot of the force produced and P_i transient for an isometric contraction (*c*), for a isovelocity stretch with no flash (*a*), and an isovelocity stretch with photogeneration of P_i (*b*). The upward pointing arrow indicates the beginning of the stretch (a sudden stretch of 38.5 μm within 2 ms (1.3% of the fiber's initial length of 2.9 mm (at sarcomere length of 2.4 μm)), followed by a steady stretch at 5% of the muscle's unloaded shortening velocity, or 0.25 mm/s. The downward directed arrow corresponds to the time at which 1 mM P_i was photogenerated. The scale at the bottom of the figure identifies the fiber's zero-force baseline, and has written on it a time scale marking the time (in s) from the laser flash. The vertical bar to the left indicates 62 kN/m^2. The oscillation of record a is the result of a small amplitude oscillation of the displacement transducer.

experiment in Fig. 9 shows that Amp_{Pi} is markedly increased by the stretch, but the k_{Pi} is little affected. When Amp_{Pi} was normalized to the force exerted before the flash, however, the results show (Fig. 10) that the relative amplitude is only modestly increased, from 13.2% to 16.6%. In this experiment k_{Pi} increased from 26.3 s^{-1} to 28.8 s^{-1}. The relative amplitude of the P_i transient increased by 13 ± 17% (mean ± SE, n = 4) and k_{Pi} was 26.9 s^{-1} ± 1.3 s^{-1} compared with the isometric control of 32.3 s^{-1} ± 2.9 s^{-1}. These results imply that at greater strains than in the isometric case, the rates governing the transitions between different force-exerting states are not significantly changed from isometric.

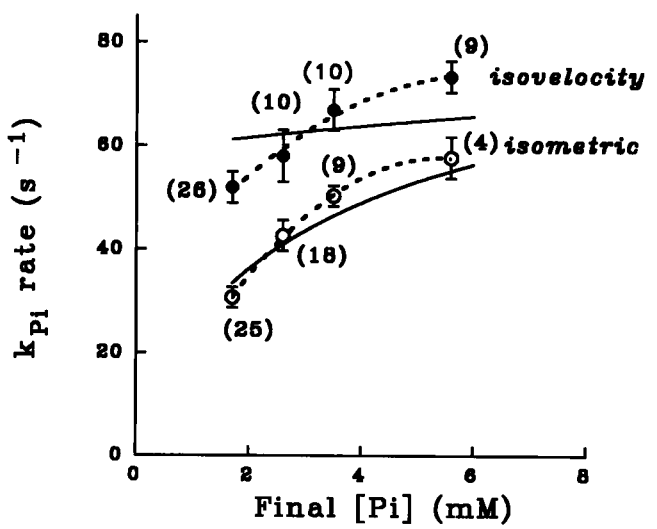

FIGURE 8 Plot of k_{Pi} as a function of the final [P_i]. The open circles are the means ± SE for isometric contractions and the closed circles are from muscles shortening at 0.1 ML/s. The solid line corresponds to the three-state strain-dependent model predictions for isometric and shortening contractions.

DISCUSSION

Basic observations

Earlier work on the cross-bridge transitions associated with P_i transients has focused on isometric contractions under different conditions; differing temperature (Dantzig et al., 1992), different degrees of activation (pCa) (Millar and Homsher, 1990; Walker et al., 1992), different types of muscle fibers (fast, slow) (Millar and Homsher, 1992), cardiac (Araujo and Walker, 1996), and contraction inhibitors (BDM) (Regnier et al., 1995) or potentiators of contraction (deoxy-ATP) (Homsher et al., 1993). Those studies show the same general pattern and support the basic conclusion that the cross-bridge cycle involves a force generating isomerization followed by the release of P_i. In addition, the rate of the force-generation step is very temperature-dependent, increasing ~fourfold for a 10°C temperature rise (Dantzig et al., 1992; Walker et al., 1991); the rate of the P_i transient is dependent on the myosin isoform type with fast-twitch fiber k_{Pi} being ~5 times faster than the cardiac k_{Pi} (Araujo and Walker, 1996), which is in turn ~5 times faster that of slow twitch muscle (Millar and Homsher, 1992). Finally, BDM inhibits the force generating isomerization (Regnier et al., 1995) while it is accelerated in fibers using deoxy-ATP as a substrate (Homsher et al., 1993). The control experiments on isometric contractions in this work confirm the previous reports in the literature

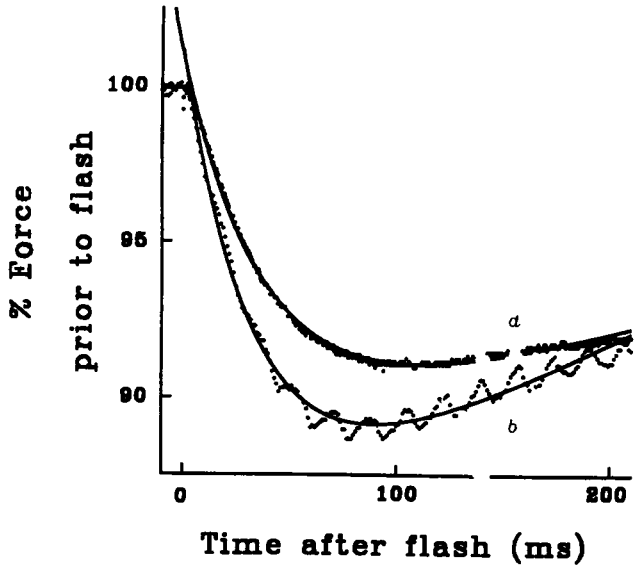

FIGURE 10 Plot of the P_i transient (*a*) of the isometric contraction in Fig. 9 (record *c*) and the P_i transient from the isovelocity stretch. In both cases the force is expressed relative to the force exerted by the fiber just before the flash. For curve *b*, the difference was measured between line a and b in Fig. 9 and normalized to the force in the muscle at the time of the flash. The dots are the experimental data, and the solid lines are least-squares fits (an exponential plus a linear baseline) for the data from 5 ms to 180 ms after the flash. The solid line in both cases is the least-squares fit to a single exponential with a sloping baseline. For recording *a* the best fit data has a st. pt. of 101.3%, amplitude of −13.2%, and a rate of 26.3 s^{-1}; for *b*, st. pt. = 101.1%, amplitude of −16.6%, and a rate of 28.8 s^{-1}.

(those cited immediately above) about the role of P_i release in the isometric cross-bridge cycle. In the current experiments, we have characterized the strain dependence of the P_i transient by either shortening or lengthening the muscle at an approximately steady state before the P_i transient or P_i perturbation. Four principal observations were made concerning strain dependence of the P_i transient.

As strain is reduced (increased shortening velocity), k_{Pi} increases in direct proportion to velocity

This result suggests that the sum of the forward and backward rates of the force generating isomerization increases as the strain on the cross-bridge is reduced. In our earlier work (Dantzig et al., 1992; Appendix) we showed that the isometric transient could be explained by assuming that the rate constant controlling the reversal of the force generation of the isomerization was independent of strain. If so, free energy considerations demand that the forward force generating isomerization must increase as cross-bridge strain or distortion is reduced. Because force declines more than stiffness during steady-state shortening (Ford et al., 1985), the strain on an attached cross-bridge during shortening is less than that in an isometric contraction. Using similar reasoning, the increased k_{Pi} during shortening might be explained. Alternatively, it could be hypothesized that the changes seen are related to the reduced force per se and not the shortening, but this hypothesis is falsified by experiments showing that when force is decreased by the reduction in Ca^{2+} or in the presence of BDM, k_{Pi} is either unchanged or reduced (Millar and Homsher, 1990; Walker et al., 1992; Regnier et al., 1995).

As shortening velocity increases, the amplitude of the P_i transient is reduced to a greater extent than steady-state force

The implication of this result is that the population of the highly strained AM.ADP is depopulated to a greater extent by the shortening than is the AM′.ADP.P_i state. This follows from the following considerations. If AM′.ADP is the only significant force-exerting state, then addition of P_i would (assuming no strain dependence P_i binding) reduce the AM′.ADP in proportion to the amount of added P_i and to the existing force. However, if there are, in addition to AM′.ADP, other force-producing states (e.g., AM′.ADP.P_i, AM) these states may not sustain as great a depopulation on shortening. As a result, the reduction in AM′.ADP by increasing the P_i will not produce as great a fall in force. On the other hand, if shortening had acted simply to speed the rate of formation of AM′.ADP, then P_i photogeneration would produce a larger amplitude change in force during shortening.

During shortening, the extent to which a given amount of P_i increases k_{Pi} is about the same as that in the isometric case (Fig. 8)

This result seems to imply that the equilibrium constant for P_i binding to the AM.ADP state is not greatly altered by changes in cross-bridge strain. This idea stems directly from Scheme II in Dantzig et al. (1992), which applies to the mechanism in which K_c is a rapid equilibrium, and where $k_{Pi} = k_a + k_b^*[P_i/(P_i + K_c)]$.

$$\text{AM.ADP.P}_i \underset{k_b}{\overset{k_a}{\leftrightarrow}} \text{AM''.ADP.Pi} \overset{K_c}{\leftrightarrow} \text{AM'.ADP} + \text{Pi}$$

(Scheme I)

If K_c decreased as a result of a decrease in strain, then k_{Pi} should increase more steeply with $[P_i]$ than in the isometric case. Similarly, if a decrease in strain produced an increase in K_c, the converse would be observed. However, in cross-bridge model simulations (see below) in which K_c is not varied with cross-bridge strain, we did not observe a parallelism of the rates as seen in Fig. 8. The explanation for this behavior is not known.

During forced lengthening, neither k_{Pi} or relative Amp_{Pi} change significantly

This result implies that the rate constants controlling the force generation and P_i release are little changed at higher

strains. This conclusion may seem contradictory to the earlier results, which imply an increase in the rate at lower strain. However, most of the force observed in the stretched muscle is produced by cross-bridges which are brought to a greater distortion by the applied stretch. As a result the transitions monitored by the P_i-jump during forced lengthening are those from cross-bridges at strains not present in isometric conditions.

Implications for the cross-bridge cycle

A comparison of these results with the experiments of Ma and Taylor (1994) on freely shortening myofibrils suggests that during rapid sarcomere shortening the rate-limiting step in the cross-bridge cycle is one immediately preceding the force-generating isomerization. Using the following model, measurements of k_{+2}, k_{-2}, actin-activated V_{max}, and P_i-burst size at 20°C were made. Reasoning from other data that steps 5 and 6 were $>500\ s^{-1}$, Ma and Taylor estimated that k_{+4} was the "effective" rate-limiting step for the ATPase cycle in freely

$$\mathrm{AM} + \mathrm{ATP} \overset{(1)}{\leftrightarrow} \mathrm{AM(ATP)} \overset{(2)}{\leftrightarrow} \mathrm{AM.ADP.Pi} \overset{(4)}{\leftrightarrow} \mathrm{AM'.ADP.P_i}$$

$$\mathrm{M.ATP} \overset{(3)\downarrow\uparrow}{\underset{2}{\leftrightarrow}} \mathrm{M.ADP.Pi} \quad \downarrow\uparrow(3)$$

$$\rightarrow \mathrm{AM.ADP} \overset{(5)}{\leftrightarrow} \mathrm{AM} \quad (6)$$

shortening myofibrils at 100 mM ionic strength and was 140 s^{-1}. This estimate assumes that 22% of the total myosin S1 heads were bound in the steady state. A similar calculation for k_{+4} can be made using their data for k_{+2}, k_{-2}, actin-activated V_{max}, and a P_i-burst of 0.35 at 40 s^{-1} at 10°C. In this case $k_{+4} = 70-80\ s^{-1}$ (again assuming a fractional myosin S-1 binding of 0.22). The relevance to the present work is that the $AM.ADP.P_i \leftrightarrow AM'.ADP.P_i$ transition (step 4) is the one probed by the P_i transient. At the relatively low shortening velocity of 0.15 V_u, k_{Pi} was 110 s^{-1} (Fig. 4), 30 s^{-1} faster than the 80 s^{-1} estimated from the data and scheme of Ma and Taylor, and it is likely that k_{Pi} is faster still at higher shortening velocities. If the force-generating isomerization and P_i release in the fiber are faster than step 4 in Ma and Taylor's reaction mechanism, *there must be a rate-limiting isomerization before the force-generating step and* P_i release. Therefore, the rate-limiting step for the cross-bridge cycle of a rapidly shortening muscle must occur during the weak-to-strong transition, but before force-generation or P_i release. (This conclusion is premised on the assumption that the Ma and Taylor scheme is correct and could change substantially if another transition is rate-limiting.) The reason P_i release per se had been suggested as the rate-limiting step for calcium control of the cycle was that a minimalist reaction sequence like the one above was used (Chalovich and Eisenberg, 1981, 1982) and no data were available regarding k_{Pi}. Additionally, in the isometric contraction, since the rate of ATP binding, cleavage, the P_i transient and P_i release, and rate of force rise are all more than 10 times greater than the isometric ATPase rate, the rate limiting step for the cross-bridge cycle must occur after the P_i release.

What molecular mechanisms produce the force changes measured in the P_i transient? Smith and Geeves (1995) have suggested a mechanism based on data from Rayment et al. (1993 a,b). In the detached S1 molecule, ADP and P_i are in the ATP binding cleft, hydrolyzed but prevented from dissociating by the structures of the upper and lower domains of the 50-kD fragment and the more distal portions of the molecule. On exposure to actin, the upper domain binds to form the "A" state, which has little or no influence on the binding of the ADP and P_i. Next, the lower domain binds to the actin and force is generated as the distal portion of the myosin rocks to a position that allows P_i to escape from its binding pocket. If the strain on the upper and lower domains is large, the probability of the change in conformation that allows P_i to escape is reduced. If force is reduced, the probability of P_i release increases.

Cross-bridge models for the P_i transient

The Pate-Cooke model

Earlier studies of k_{Pi} in isometric contractions showed they could be described by a linear sequential step reaction mechanism like those used in solution biochemistry (Dantzig et al., 1992; Millar and Homsher, 1990; Walker et al., 1992; Regnier et al., 1995; Araujo and Walker, 1996). This approach may be reasonable for the isometric case, assuming that the distribution of cross-bridge strains can be approximated as some "mean" strain. The results obtained here require a strain-dependent model to account for the length changes and the consequences thereof. The Pate and Cooke model (1989a) uses strain dependency but makes force generation coincident to P_i release from the AM.ADP.P_i state. We programmed the Pate-Cooke model to examine its predictions about the P_i transients. It predicts a strictly linear decline in force with increases in log [P_i] with a slope of −18% per decade increase in [P_i]. The Pate and Cooke model also predicts a P_i transient whose behavior differs from that observed in these and earlier experiments in several important respects: 1) for a step increase in [P_i] the model predicts an *immediate* force decline as opposed to the 1–4-ms lag observed in experiments; 2) the predicted time course of force decline following a step increase in [P_i] from 1 to 2 mM in an isometric contraction can be roughly approximated by an exponential decay whose rate is 235 s^{-1} as opposed to ~30 s^{-1} observed at 10°C. The force decline is much better fit by three exponentials ranging from 80 to 1700 s^{-1}; 3) as [P_i] is increased, the predicted k_{Pi} increases practically linearly by ~200 s^{-1} per decade, compared with the asymptote of ~100 s^{-1} seen experimentally; 4) the rate of rise of force in this model starting with all the

cross-bridges detached and equilibrated between M.ATP and M.ADP.P_i is well-fit by a double exponential whose rates are 68 s^{-1} (for the initial 65% of the force rise) and 17 s^{-1} compared with the 12–23 s^{-1} observed in a number of studies (Brenner, 1986; 1988; Millar and Homsher, 1990; Metzger and Moss, 1990; Walker et al., 1992) at 10°-15°C. Nevertheless, the Pate-Cooke model's predictions are in the right general direction, which is remarkable inasmuch as the model antedates the existence of these data.

The Dantzig et al. model

We next examined a strain-dependent model in which the force-generating step precedes the P_i release. To facilitate computation and to test its success in accounting for the isometric P_i transients, we used the simple three-state model described in the Appendix of the paper by Dantzig et al. (1992) to learn to what extent it predicts the four main observations made above. In this model the following reaction scheme below was used:

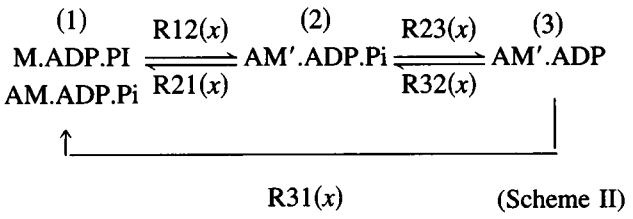

(Scheme II)

where M.ADP.P_i and AM.ADP.P_i are weakly bound or detached cross-bridges (state 1), AM'.ADP.P_i is a force exerting cross-bridge state (state 2), and AM'.ADP is also a force exerting cross-bridge state (state 3) from which P_i has dissociated. R12(x), R21(x), etc. are the rate constants that describe the transitions between states and are strain-dependent (i.e., their value depends on the value of x, the distortion of the cross-bridge from its equilibrium position ($x = 0$) where no force is exerted). In this approach we used the same basic equations as in the Dantzig et al. (1992) Appendix and computed the cross-bridge distribution over the range from −2 nm to 10 nm cross-bridge strain (the range was divided into 480 0.025-nm bins). The differential equations describing the rate of change of states 1–3 were written and numerically solved for each bin. For the model computations we assumed that the cross-bridge stiffness, k, of 0.2 RT/nm^{-2} or (8×10^{-4} N/m). We assume that the free energy content (G) of states 1–3 is

$$\begin{aligned} G_1 &= 0 \text{ kJ} \\ G_2 &= (-2.5 + k^*x^2/2) \text{ kJ} \\ G_3 &= (-2.5) + RT^*\ln(P_i/K_c) + k^*x^2/2) \text{ kJ} \end{aligned} \tag{2}$$

where K_c is 10 mM and strain-independent. Since $R_{ij}[x]/R_{ji}[x] = \exp([G_i[x]-G_j[x]]/RT)$ (where i corresponds to the state from which the reaction is proceeding and j the state to which the reaction is proceeding), we next defined the values of one of the rate constants for each step of the reaction mechanism. We assumed that the rate of P_i release (R23(x)) was fast (>500 s^{-1} at all cross-bridge distortions). R31(x) was given a value of 4 s^{-1} for $x > 0$ to provide a reasonable isometric ATPase rate (~1 s^{-1}) at 10°C. A much larger value for R31(x) was needed at $x < 0$ to obtain a realistic unloaded shortening velocity. If R31(x) is 870 s^{-1}, an unloaded shortening velocity of ~2300 nm/hs/s is obtained. Finally, Dantzig et al. (1992) found that reasonable isometric k_{Pi} fits were obtained if the reverse of the cross-bridge isomerization (R21(x)) was set to 100 s^{-1} for positive values of x, and because it is generally assumed that the cross-bridge does not readily attach at negative strains, we set R12(x) = 0.06 s^{-1} for $x < 0$. By using these assignments the isometric P_i-transient could be calculated with the results presented in Fig. 14. of Dantzig et al. (1992).

To compute a P_i transient during shortening, we first computed the steady-state cross-bridge distribution at each value of x at a particular shortening velocity, and from it the isovelocity force. This was done by starting with the cross-bridge distribution in the isometric case. Shortening at a particular velocity was represented by a series of small step-wise displacements of cross-bridges at one value of x to a smaller value of x; i.e., if the muscle is shortening at 100 nm/hs/s (0.092 ML/s), shortening is represented as a series of 0.025 nm displacements every 250 μs. After steady-state force was reached, the cross-bridge distribution was stored. The rate constant R32(x) was altered by increasing [P_i] in the equation for G_3, and the computation of the P_i transient during simulated shortening continued using the steady-state shortening cross-bridge distribution as the initial conditions and the altered G_3. The results of the computations using this procedure are similar to those seen in the inset to Fig. 11. The model predicts that during shortening k_{Pi} will increase and the transient amplitude does decrease out of proportion to the change in steady-state force. However, using the rates above, k_{Pi} for a P_i jump from 1 to 2 mM, k_{Pi} is two- to threefold faster than and the amplitudes were less than half of those observed experimentally. Examination of the reasons for these high rates showed that during shortening the largest tension changes occurred at cross-bridge distortions ~0.5–1.0 nm less than in the comparable isometric case. The value of R12(x) at these strains was too large (set by free energy considerations and the value of R21(x)). To reduce the rates of the isovelocity transients it was necessary to reduce the value of R21(x) at distortions <6 nm. We therefore altered the rates of R12(x) (letting R21(x) change as set by free-energy considerations), recomputed the isometric and shortening k_{Pi}, and further adjusted R12(x) if necessary. Using this iterative process we found that reasonable behavior could be obtained using a Gaussian function of x for R12(x) (see Fig. 11 for plots of the strain-dependence of each rate constant).

The predictions of this model and associated rates are given in the Figs. 4, 5, and 8 by the solid lines. The model successfully predicts the size of the phosphate dependency of isometric force and it exhibits a subtle sigmoidal rela-

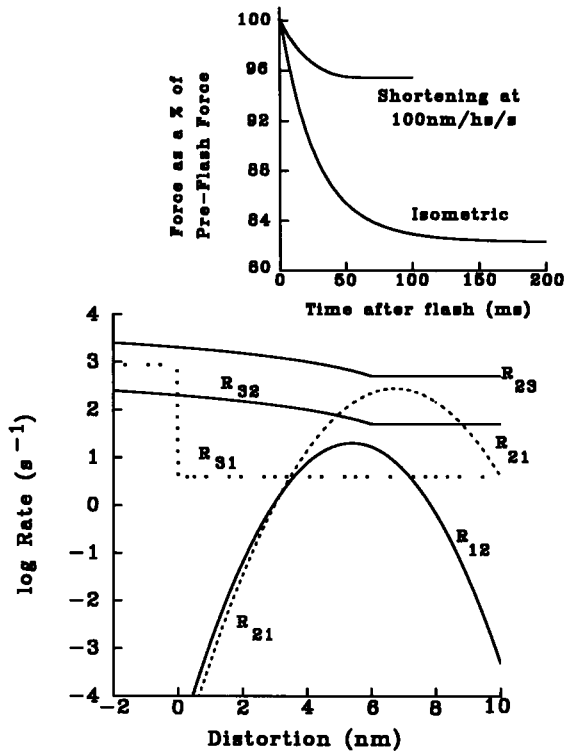

FIGURE 11 A plot of the rate constants used in the strain-dependent model that produced the predictions given by the dotted lines in Figs. 4, 5, and 8. The inset is a model-generated P_i transient (P_i increases from 1 to 2 mM at zero time) for the isometric case (*i*) and for shortening at 100 nm/hs/s. Note the reduced amplitude and more rapid decay in force seen in the shortening simulation. k_{Pi} for the isometric case is 36 s^{-1} and for the isovelocity case is 55.4 s^{-1}. The amplitude for the isometric simulation is −18.0% and for the isovelocity is −5.0% of the preflash values.

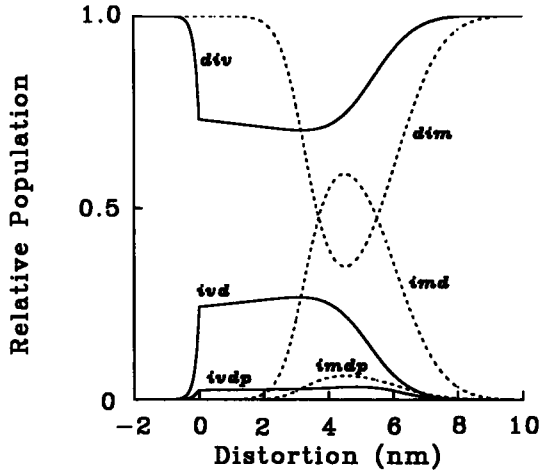

FIGURE 12 A plot of the fractional distribution of the cross-bridge intermediates at various strains for an isometric contraction (*im*) at steady state (*dotted lines*) and for isovelocity shortening (*iv*) at 100 nm/hs/s (*solid lines*). *dim* and *div* correspond to the detached isometric and isovelocity intermediate (M.ADP.P_i) respectively; *imdp* and *ivdp* to the isometric and isovelocity AM.ADP.P_i state respectively; and *imd* and *ivd* to the isometric and isovelocity AM.ADP states respectively.

tionship between isometric force and log [P_i] as reported earlier in Dantzig et al. (1992, Fig. 13 *C*). Linear regression of the isometric force predicted by the model at 0.2, 1.0, 2.0, 5.0, 10, and 20 mM [P_i] against log [P_i] yields a straight line whose slope is −36.5% per decade [P_i] and whose coefficient of determination is 0.976. The magnitude of the deviation of the force values from a straight line predicted by the model at 0.2 and 20 mM would be difficult to detect experimentally unless one specifically looked for them. This distribution of rate constants (R12(*x*), etc.) successfully predicts the isometric k_{Pi} rates (Fig. 8), and was similar to both the rates and amplitudes for the P_i steps from 0.7 mM to 1.7 mM at shortening velocities ranging from −25 nm to 222 nm per half sarcomere per second (see Figs. 4 and 5). Representative time courses of predicted P_i-transients for isometric and isotonic (100 nm/hs/s) contractions are given in the inset to Fig. 11 and show that the predicted transients are exponential. These transients also exhibit a several-ms lag, and it does not change in any consistent way as the [P_i] increases (Dantzig et al., 1992). At higher P_i concentration *and* during shortening at speeds >50 nm/hs/s, the computed P_i transient is not as well fit by a single exponential. This was shown by regular oscillation of the residuals about zero, and suggests the need to fit the data with several exponentials. However, we do not regard this behavior as a serious shortcoming because examination of Figs. 3 and 7 show that at the higher speed and at higher [P_i] there is an increased scatter of the data about the fit arising from the reduced signal-to-noise ratio seen under these conditions.

Using the strain-dependencies in Fig. 11, we computed the time course of force development starting with all the cross-bridges detached. The model predicts an exponential rise of force whose rate constant is dependent on [P_i] (increasing with and increase in [P_i]). At 1 mM P_i, the rate of rise of force was monoexponential at 20 s^{-1} and is similar to the results of earlier studies that find the rate of rise of force, k_{tr}, ranges from ~12–23 in the temperature range 10–15°C (Brenner, 1986; Metzger and Moss, 1990; Millar and Homsher, 1990). As [P_i] increases, the rate of rise of force increases (reaching 31 s^{-1} at 10 mM) and the time course is better fit by two exponentials at higher [P_i].

The major discrepancy between the model predictions and experiment is the dependency of k_{Pi} on [P_i] during shortening at 111 nm/hs/s (Fig. 8). The model predicts a slope to the relationship that is ~15% of the observed slope. The model predictions can be brought better in line with the data in Fig. 8 by making K_c strain-dependent (decreasing it with decreased strain). However, in solution, AM.ADP binds P_i very weakly ($K_c \gg 10$ M) (Geeves et al., 1984). To use a strain dependence of K_c to better fit the shortening data in Fig. 7, one must postulate that at strains >5 nm K_c does not change, at strains <5 nm, K_c falls to values near 1–2 mM, and at strains near 0 nm, K_c rises to >1M. This scenario seems unlikely and the reasons for the discrepancy remain unresolved.

The Effect of Series Elasticity

In model simulations, Luo et al. (1993) showed that the introduction of series compliance into cross-bridge models could markedly reduce the rate of the observed force transients resulting from the photogeneration of ATP in a rigor fiber or P_i in a contracting fiber. Further addition of series compliance beyond that in the cross-bridge markedly reduces the change in stiffness that accompanies such transients, because the change in stiffness is shared between the cross-bridge and the series compliance. Recent measurements showing that the thin filament contributes ~50% to the compliance of the muscle fiber at maximal overlap (Higuchi et al., 1995), raise the question of the extent to which the results here are influenced by the series compliance. In paired comparisons of k_{Pi} measured at 2.5 μm with those at 3.3 μm (at which the series compliance of the actin should increase relative to that of the cross-bridge), Dantzig et al. (1992) found no significant differences in the k_{Pi}. Furthermore, Dantzig et al. (1992) measured the change in stiffness accompanying phosphate transients and found that the relative change in stiffness was 85% of that of force. These observations suggest that while series compliance is likely to play a significant role in the observed values for k_{Pi}, definition of its role requires additional experimentation.

Finally, the model's behavior for eccentric contractions at speeds more negative than −25 nm/hs/s are not reflective of muscle behavior; i.e., the model predicts that force will rise to ~1.75× the isometric force and then progressively fall to steady-state values less than the initial isometric value. Only at velocities more positive than −25 nm/hs/s does force rise to and remain at values ~1.3 that of isometric. The problem could be remedied by increasing the rate of force generation at strains >6 nm. More experimentation is needed to better characterize this type of contraction.

This model does not fully explain the phosphate transient. The model more closely fits the observed transient behavior than the Pate and Cooke model in that the decline in force is well approximated by a single exponential, the model provides a small lag at the beginning of the transient, and the rates and amplitudes of the transients are appropriate. Thus the inclusion of a force-generating isomerization preceding P_i release better predicts the behavior seen in P_i transients (Millar and Homsher, 1990; Fortune et al., 1991; Kawai and Halvorson, 1991). Part of the reason for this is that it reduces the dependency of the P_i transient rate on the free energy change for the P_i release step. When the P_i release step per se produces the force, the absolute rates of the release and binding vary over a much larger range, which causes the P_i transient to be very fast and multiexponential. More elaborate models, however, will be required to better fit the data. Nevertheless, the information from P_i transients during shortening and forced lengthening should be useful in defining the strain dependence of the rates into and out of the force-bearing states.

The authors gratefully acknowledge Drs. P. B. Chase, J. Dantzig, and M. Geeves, and C. Morris, for useful discussions of the experiments.

This work was supported by the National Institute of Arthritis and Musculoskeletal and Skin Diseases Grant AR30988 (to E.H.).

REFERENCES

Araujo, A., and J. Walker. 1996. Phosphate release and force generation in cardiac myocytes investigated with caged phosphate and caged calcium. *Biophys. J.* 70:2316–2326.

Brenner, B. 1986. The crossbridge cycle in muscle: mechanical, biochemical, and structural studies on single skinned rabbit psoas fibers to characterize cross-bridge kinetics in muscle for correlation with actomyosin-ATPase in solution. *Basic Res. Cardiol.* 81:1–15.

Brenner, B. 1988. Effect of Ca^{2+} on cross-bridge turnover kinetics in skinned single rabbit psoas fibers: implications for regulation of muscle contraction. *Proc. Natl. Acad. Sci. USA.* 85:3265–3269.

Chalovich, J. M., and E. Eisenberg. 1981. Inhibition of actomyosin ATPase activity by troponin-tropomyosin without blocking the binding of myosin to actin. *J. Biol. Chem.* 257:2432–2437.

Chalovich, J. M., and E. Eisenberg. 1982. Inhibition of actomyosin ATPase activity by troponin without blocking binding of myosin to actin. *J. Biol. Chem.* 257:2432–2437.

Dantzig, J., Y. Goldman, N. Millar, J. Lacktis, and E. Homsher. 1992. Reversal of the cross-bridge force-generating transition by photogeneration of phosphate in rabbit psoas muscle fibers. *J. Physiol. (Lond.).* 451:247–278, 1992.

Edman, K. A. P. 1979. The velocity of unloaded shortenings and its relation to sarcomere length and isometric force in vertebrate muscle fibers. *J. Physiol. (Lond.).* 291:143–159.

Eisenberg, E., T. Hill, and Y. Chen. 1980. Cross-bridge model of muscle contraction. *Biophys. J.* 29:195–227.

Ford, L. E., A. F. Huxley, and R. M. Simmons. 1977. Tension responses to sudden length change in stimulated frog muscle fibers near slack length. *J. Physiol. (Lond.).* 269:441–515.

Ford, L. E., A. F. Huxley, and R. M. Simmons. 1985. Tension transients during steady state shortening of frog muscle fibers. *J. Physiol. (Lond.).* 361:131–150.

Fortune, P., M. Geeves, and K. Ranatunga. 1991. Tension responses to rapid pressure release in glycerinated rabbit muscle fibers. *Proc. Natl. Acad. Sci. USA.* 88:7323–7327.

Fortune, N., M. Geeves, and K. Ranatunga. 1994. Contractile activation and force generation in skinned rabbit muscle fibers: effects of hydrostatic pressure. *J. Physiol. (Lond.).* 474:283–290.

Geeves, M., R. Goody, and H. Gutfreund. 1984. Kinetics of acto-S1 interactions as a guide to a model for the crossbridge cycle. *J. Muscle Res. Cell Motil.* 5:351–361.

Goldman, Y. E., M. G. Hibberd, and D. R. Trentham. 1984. Relaxation of rabbit psoas muscle fibres from rigor by photochemical generation of adenosine-5'-triphosphate. *J. Physiol. (Lond.).* 354:577–604.

Hibberd, M., J. A. Dantzig, D. R. Trentham, and Y. E. Goldman. 1985. Phosphate release and force generation in skeletal muscle fibers. *Science.* 228:1317–1319.

Higuchi, H., T. Yanaguida, and Y. Goldman. 1995. Compliance of thin filaments in skinned fibers of rabbit skeletal muscle. *Biophys. J.* 69: 1000–1010.

Homsher, E., and J. Lacktis. 1988. The effects of shortening on the phosphate release step of the actomyosin ATPase mechanism. *Biophys. J.* 53:564*a*. (Abstr.).

Homsher, E., and J. Rall. 1973. Energetics of shortening muscles in twitches and tetanic contractions. I. A reinvestigation of Hill's concept of a shortening heat. *J. Gen. Physiol.* 629:663–676.

Homsher, E., M. Regnier, and S. Tejeda. 1993. The effect of ATP analogs (NTP) on thin filament movement in motility assays and on the phosphate transient in rabbit glycerinated skeletal muscle fibers. *Biophys. J.* 64:250*a*. (Abstr.).

Kawai, M., and H. Halvorson. 1991. Two-step mechanism of phosphate release and the mechanism of force generation in chemically skinned fibers of rabbit psoas muscle. *Biophys. J.* 59:329–342.

Kawai, M., and Y. Zhao. 1993. Cross-bridge scheme and force per cross-bridge state in skinned rabbit psoas muscle fibers. *Biophys. J.* 65:638–651.

Knight, P., N. Fortune, and M. Geeves. 1993. Effects of pressure on equatorial x-ray diffraction from skeletal muscle fibers. *Biophys. J.* 65: 814–822.

Luo, Y., R. Cooke, and E. Pate. 1993. A model of stress relaxation in cross-bridge systems: effect of a series elastic element. *Am. J. Physiol.* 265:C279–C288.

Ma, Y., and E. Taylor. 1994. Kinetic mechanism of myofibril ATPase. *Biophys. J.* 66:1542–1553.

Metzger, J., and R. Moss. 1990. Calcium-sensitive crossbridge transition in mammalian fast and slow skeletal muscle fibers. *Science.* 247: 1088–1090.

Millar, N. C., and E. Homsher. 1990. The effect of phosphate and calcium on force generation in glycerinated rabbit skeletal muscle fibers. *J. Biol. Chem.* 265:20234–20240.

Millar, N., and E. Homsher. 1992. Kinetics of force generation and phosphate release in skinned rabbit soleus muscle fibers. *Am. J. Physiol.* 262:C1239–C1245.

Pate, E., and R. Cooke. 1989a. A model of crossbridge action: the effects of ATP, ADP, and Pi. *J. Mus. Res. Cell Motil.* 10:181–196.

Pate, E., and R. Cooke. 1989b. Addition of phosphate to active fibers probes actomyosin states within the powerstroke. *Pflugers Arch. Eur. J. Physiol.* 414:73–81.

Press, W. H., B. P. Flannery, S. A. Teukolsky, and W. T. Vetterling. 1986. Numerical Recipes. Cambridge University Press, Cambridge, UK. 498–528.

Rayment, I., H. Holden, M. Whittaker, C. Yohn, M. Lorenz, K. Holmes, and R. Milligan. 1993a. Structure of the actin-myosin complex and its implications for muscle contraction. *Science.* 261:58–65.

Rayment, I., W. Rypniewski, K. Schmidt-Base, R. Smith, D. Tomchick, M. Menning, D. Winkelman, G. Wesenberg, and H. Holden. 1993b. Three-dimensional structure of myosin subfragment-1: a molecular motor. *Science.* 261:50–58.

Regnier, M., C. Morris, and E. Homsher. 1995. Regulation of the cross-bridge transition from a weakly to strongly bound state in skinned rabbit muscle fibers. *Am. J. Physiol.* 269:C1532–C1539.

Sleep, J., and R. Hutton. 1978. Actin medicated release of ATP from myosin ATP-complex. *Biochemistry.* 17:5417–5422.

Smith, D., and M. Geeves. 1995. Stain-dependent cross-bridge cycle for muscle. *Biophys. J.* 69:524–537.

Walker, J. W., Z. Lu, and R. L. Moss. 1992. Effects of Ca^{2+} on the kinetics of phosphate release in skeletal muscle. *J. Biol. Chem.* 267:2459–2466.

White, H. D., and E. W. Taylor. 1976. Energetics and mechanism of actomyosin ATPase. *Biochemistry.* 15:5818–5826.

Woledge, R. C., N. A. Curtin, and E. Homsher. 1985. Energetic Aspects of Muscle Contraction. Academic Press, London.

Zhao, Y., and M. Kawai. 1994. Kinetic and thermodynamic studies of the cross-bridge cycle in rabbit psoas muscle fibers. *Biophys. J.* 67: 1655–1668.